ELSEVIER

Journal of Non-Crystalline Solids 222 (1997) 167–174

JOURNAL OF NON-CRYSTALLINE SOLIDS

# Effects of glass structure on the corrosion behavior of sodium-aluminosilicate glasses

James P. Hamilton, Carlo G. Pantano*

*Department of Materials Science and Engineering, The Pennsylvania State University, University Park, PA 16802, USA*

**Abstract**

The leaching and dissolution behavior of two sodium-aluminosilicate glasses, with structures containing one versus five non-bridging oxygen sites per 10 tetrahedra, is discussed for both acid (pH 2) and base (pH 9) reactions. The soda concentration was held constant at 25 mol%. X-ray photoelectron spectroscopy, secondary ion mass spectroscopy and Fourier transform infrared reflection spectroscopy have been used to determine the composition and structure of the reacted glass surfaces. The glass with five NBO sites per 10 tetrahedra exhibits extensive surface layer formation in both acid and base. Conversely, the glass with one NBO site per 10 tetrahedra exhibits total dissolution in acid; in base, this glass is essentially unreactive. © 1997 Elsevier Science B.V.

## 1. Introduction

The aqueous corrosion behavior of sodium-aluminosilicate glasses is related to the concentration of non-bridging oxygen (NBO) sites in the glass network structure; in this system, the NBO concentration is a direct function of the alumina content. The concentration of NBO sites influences the reaction rate with $H_2O$, $H^+$ and $H_3O^+$ as well as the diffusivity of water and modifier ions. The alumina, itself, also influences the corrosion behavior because it introduces new sites for hydrolysis reactions, i.e. Al–O–Si, Al–O–Al, and $(AlO_4)^-$ $Na^+$ sites. This concept is often employed to control the chemical durability of soda-lime-silicate glasses through the addition of small amounts of alumina [1]. Also, chemically durable sodium-aluminosilicate glasses provide excellent matrices for the immobilization of radioactive fission products [2]. In a more general sense, the dissolution behavior of amorphous and crystalline alkali-aluminosilicates is extremely important in the field of mineral/water interface

* Corresponding author. E-mail: pantano@ems.psu.edu

0022-9093/97/$17.00 
*PII* S0022-3093(97)00395-5

geochemistry; environmental models used to make groundwater and soil porewater chemical predictions depend, fundamentally, upon the dissolution mechanisms of aluminosilicate minerals and glassy phases within them.

The corrosion behavior of alkali-silicate glasses in water has been investigated in detail over the past few decades. From these investigations, a few theories have been proposed to model the hydration and leaching behavior of alkali-silicate glass. Doremus [3] proposed an ion exchange model that involves the interdiffusion of hydrogen (or hydronium) ions from the water and alkali ions in the glass. In the case of sodium, the exchange reaction has the form: $\equiv SiO^- Na^+ + H_3O^+ \rightarrow \equiv SiO^- H_3O^+ + Na^+OH^-$ [3]. This theory was the only accepted model until Smets and Lommen [4] proposed a new mechanism in which leaching of alkali ions in near-neutral conditions is controlled by the diffusion of molecular water into the glass network. As molecular water diffuses into the glass network, it becomes immobilized at alkali-NBO sites by the formation of silanol groups. This process results in charge compensation and the mobilization of alkali ions, which then diffuse to the glass/water interface with their hydroxyl co-ions. The rate-limiting step is the diffusion of molecular water into the glass network, and is described by the following reaction: $\equiv SiO^- Na^+ + H_2O \rightarrow \equiv SiOH + Na^+OH^-$ [4]. Other models have since been developed which incorporate both mechanisms [5,6].

It is widely accepted that the presence of alumina results in the bonding of Na ions to both $AlO_4^-$ tetrahedra (or $AlO_6^{3-}$ octahedra) and non-bridging oxygens [7–12]. However, Smets and Lommen [12] have suggested that all NBO sites disappear at an $Al/Na < 1$ (at which point all of the sodium ions bond to the aluminate species) versus the more widely accepted value of $Al/Na = 1$ [7–11]. In another paper [13], Smets and Lommen concluded that Na ions bonded to non-bridging oxygens are more easily leached than Na ions bonded to the aluminum part of the network. Penetration of molecular water into the glass network does not neutralize the negatively charged $AlO_4^-$ tetrahedra and therefore, does not mobilize Na ions bonded to these tetrahedra. These Na ions are leached by the ion exchange process described by Doremus [3], which occurs at a much slower rate than the diffusion of molecular water. Smets and Lommen [13] also suggested that the presence of small quantities of alumina in the glass network is sufficient to completely block the paths along which molecular water diffuses and causes a significant decrease in the diffusion coefficient of molecular water.

It is the aim of this research to further investigate the relationship between the concentration of NBO sites in the sodium-aluminosilicate glass network structure and corrosion behavior by studying their behavior in both acidic and basic solutions. Further, this investigation includes characterization of the composition and structure of layers that form on these glass surfaces during corrosion. The relationship between surface layer formation and bulk glass structure is of specific interest. X-ray photoelectron spectroscopy (XPS), secondary ion mass spectrometry (SIMS), and Fourier transform infrared reflectance spectroscopy (FTIRRS) were used to study the composition and structure of the glass surfaces. Inductively coupled plasma spectrometry (ICP) was used to monitor the dissolution rate of the glasses.

The compositions of the sodium-aluminosilicate glasses investigated are shown in Fig. 1. In the $Na_2O$–$xAl_2O_3$–$(3-x)SiO_2$ system, the glass network structure can be systematically altered by substituting alumina for silica, while maintaining a constant soda concentration. This procedure systematically changes the concentration of NBO sites and facilitates the investigation of corrosion behavior as a function of glass structure, and not soda concentration. The corrosion behavior of glasses with the compositions $Na_2O$–$0.2Al_2O_3$–$2.8SiO_2$ and $Na_2O$–$0.8Al_2O_3$–$2.2SiO_2$ will be discussed here. These glasses will be referred to as '0.2 glass' and '0.8 glass', respectively.

## 2. Experimental procedures

### 2.1. Sample preparation

The 0.2 and 0.8 glasses were prepared from Min-U-Sil $SiO_2$, reagent-grade $Al(OH)_3$, anhy-

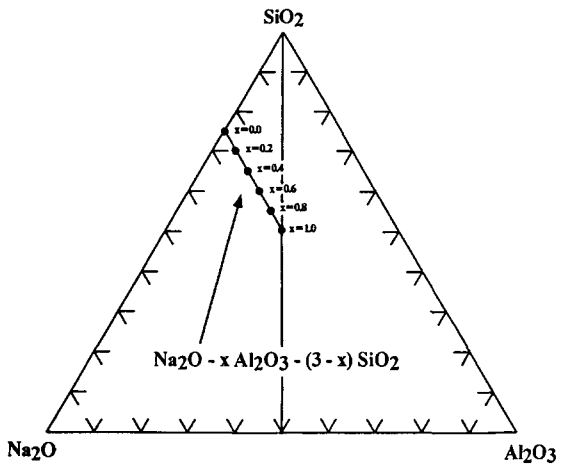


Fig. 1. $Na_2O$–$Al_2O_3$–$SiO_2$ ternary phase diagram illustrating the $Na_2O$–$xAl_2O_3$–$(3-x)SiO_2$ glass system.

drous $Na_2CO_3$, and $Na_2SO_4$ powders. Batches of 150 g of the 0.2 and 0.8 compositions were melted in platinum crucibles at 1550 and 1600°C in air, respectively. The glasses were melted for 24 h and then poured into graphite molds to form either rods or plates. The 0.2 and 0.8 glasses were annealed overnight at 520 and 650°C, respectively, and then cooled slowly to room temperature. Table 1 presents spectrochemical analyses of these glasses and indicates minor deviation from their batch compositions.

Plates ~ 2 cm long × 1 cm wide × 0.2 cm thick were cut and one face was polished to 0.1 μm grit size with oil-based diamond sprays and a final 0.05 μm cerium oxide/chrome oxide polishing step. After polishing, the samples were rinsed in acetone and hydrocarbons were removed by a 30-min ultraviolet ozone cleaning (UVOC) process. Finally, the 0.2 and 0.8 glasses were etched in 1 N NaOH solution at 80°C for 20 s and 3 min, respectively, to remove the damaged/contaminated surface layer due to polishing. The samples were immediately rinsed in deionized water at 80°C following the etch. Before exposure to aqueous solutions, the samples were treated by UVOC again for 30 min. This surface preparation procedure yields a clean, smooth, glass surface with a surface composition similar to that of the bulk glass.

Table 1
Spectrochemical analyses of 0.2 and 0.8 glasses

| | $Na_2O$ (mol%) | $Al_2O_3$ (mol%) | $SiO_2$ (mol%) |
|---|---|---|---|
| $Na_2O$–$0.2Al_2O_3$–$2.8SiO_2$ | | | |
| Batch composition | 25.0 | 5.0 | 70.0 |
| Spectrochemical analysis | 26.0 | 5.2 | 68.8 |
| $Na_2O$–$0.8Al_2O_3$–$2.2SiO_2$ | | | |
| Batch composition | 25.0 | 20.0 | 55.0 |
| Spectrochemical analysis | 25.1 | 20.0 | 54.9 |

The polished glasses were placed in polyfluorotetraethylene (PTFE) baskets that hang vertically from the top of 2-l high-density polyethylene (HDPE) containers. These containers were precleaned in hydrochloric acid, nitric acid, and boiling water in order to create as sterile an environment as possible. Acid solutions with a pH of 2 were prepared with trace metal HCl and deionized water. Base solutions with a pH of 9 were prepared by dissolving LiOH crystals in deionized water. The terms acid and base will be used to refer to the pH 2 and pH 9 solutions, respectively, in which the experiments were conducted. The glass specimens were immersed in these solutions for up to 1000 h and the solution was never replenished. The containers were placed in a standard oven which maintained a temperature of 25 ± 1°C. The sample surface area to solution volume ratio (SA/V) was ~ $5.0 \times 10^{-3}$ $cm^{-1}$ for each experiment.

### 2.2. Sample characterization

The compositions of the outermost 100 Å of the glass surfaces were measured with XPS using a Kratos XSAM 800 spectrometer. Non-monochromatic, Mg Kα X-rays were used with an anode current of 20 mA at an electron acceleration voltage of 14 kV. The pass energy was set at 40 eV and the analyzed area was ~ 1 mm in diameter. The compositions of the glass surfaces were determined from high resolution scans of the Na KLL, C 1s, O 1s, Al 2p, and Si 2p peaks. The collection time for each peak was adjusted to yield a signal/noise ratio of at least 50/1.

Depth profiles of the glass surfaces were obtained with SIMS using a Cameca IMS/3F spectrometer. A 250 nA, 14.5 keV, $^{18}O^-$ primary beam was used. A 150-μm diameter spot was rastered over a 250 × 250 μm area. Positive secondary ions were collected over a 10-μm diameter area in the center of the crater. The glass surfaces were not coated; a gold TEM grid provided sufficient surface charge stabilization. These conditions resulted in a sputtering rate of 150 Å/min.

FTIR reflectance spectra were obtained with a Bruker 113 V spectrometer. The analyses were performed in vacuum over a range of 4000–400 $cm^{-1}$ with a specular reflectance attachment.

## 3. Results

### 3.1. $Na_2O$–0.2$Al_2O_3$–2.8$SiO_2$

The surface compositions of the 0.2 glasses, as measured with XPS, are presented in Fig. 2; Na/Si and Al/Si atomic percent ratios are plotted as a function of leaching time in both acidic and basic solutions. The Na/Si and Al/Si ratios measured for the unleached glass surface are indicated by asterisks at the left-hand side of Fig. 2. The data indicate time-dependent sodium depletion and some aluminum depletion in the glass surfaces leached in acid. The glass surfaces leached in base exhibit less sodium depletion than in acid, and no detectable aluminum depletion. (Note: the Na/Si ratio for the unleached glass is slightly lower than the bulk ratio due to some degree of sodium depletion during the final stages of sample preparation.)

The FTIRR spectra for the 0.2 glass leached in acid are plotted in Fig. 3 over the range of 1350–550 $cm^{-1}$. The spectra have been off-set to clearly illustrate any shape changes and shifts of each peak. The peak at ≈1060 $cm^{-1}$ in the unleached glass is attributed to the stretching vibration of the Si–O–Si bonds (bridging oxygens). A second peak, associated with the stretching vibration of Si–O-modifier bonds (non-bridging oxygens), is located at ≈980 $cm^{-1}$ in the unleached glass [14]. In the 0.2 glass, this peak is associated with non-bridging oxygens created by the presence of Na modifiers in the network. As leaching time increases, the Si–O–Si peak shifts to higher wavenumbers and the Si–O-modifier peak shifts to lower wavenumbers and decreases in intensity. Also, the shoulder located a few wavenumbers higher than the Si–O–Si peak becomes more pronounced and shifts to higher wavenumbers with increasing leaching time. These effects indicate the formation of a surface layer whose structure differs from the bulk glass [14].

Fig. 4 illustrates surface layer formation in terms of the FTIRR spectra for the 0.2 glasses

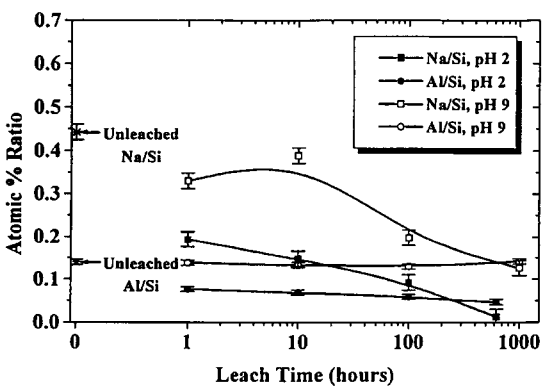


Fig. 2. XPS Na/Si and Al/Si atomic percent ratios as a function of leaching time for $Na_2O$–0.2$Al_2O_3$–2.8$SiO_2$ glasses leached in pH 2 and pH 9 solutions at 25°C. Lines are drawn as guides for the eye.

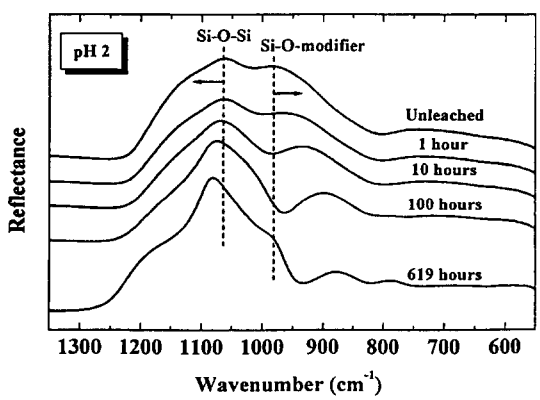


Fig. 3. FTIRR spectra of $Na_2O$–0.2$Al_2O_3$–2.8$SiO_2$ glasses leached in pH 2 solution at 25°C for up to 619 h.

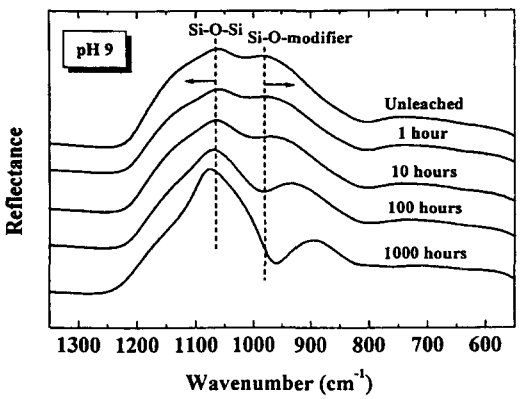


Fig. 4. FTIRR spectra of $Na_2O$–$0.2Al_2O_3$–$2.8SiO_2$ glasses leached in pH 9 solution at 25°C for up to 1000 h.

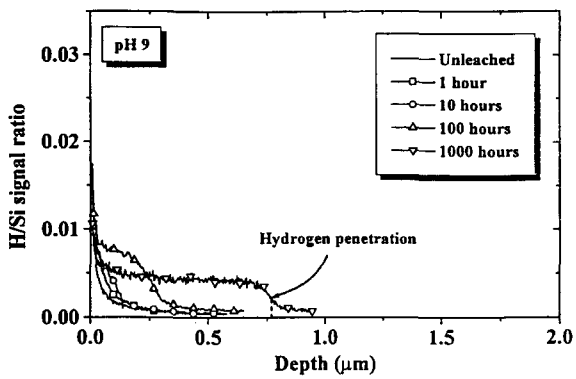


Fig. 6. SIMS hydrogen depth profiles of $Na_2O$–$0.2Al_2O_3$–$2.8SiO_2$ glasses leached in pH 9 solution at 25°C for up to 1000 h.

leached in base. Note that the formation of the surface layer in base occurs at a rate that is one order of magnitude slower than in acid.

Hydrogen depth profiles of the 0.2 glasses leached in acid are shown in Fig. 5. These profiles are plotted as the H/Si secondary ion signal on the ordinate vs. depth on the abscissa. The sharp interface indicated by the sudden drop in the H/Si ratio, provides an excellent marker for the penetration depth of hydrogen into the glass surface. The hydrogen penetration depth is defined by the point where the ratio drops by 50% in the interface region. The sodium profiles (not shown here) of these glasses indicate a sodium depletion at the surface that gradually rises to the bulk. Fig. 6 illustrates the hydrogen profiles for the glasses leached in base. The penetration of hydrogen into the glass surface in base occurs at a slower rate than in acid.

Analysis of the profiles in Figs. 5 and 6 indicate that the inward diffusion of hydrogen (as $H^+$, $H_3O^+$, or $H_2O$) and the corresponding outward diffusion of sodium follow parabolic kinetics in both acid and base (see below). The aluminum and silicon profiles in the glasses leached in acid and base were the same as the profiles in the unleached glass. ICP solution analyses of the acid and base solutions did not detect the presence of

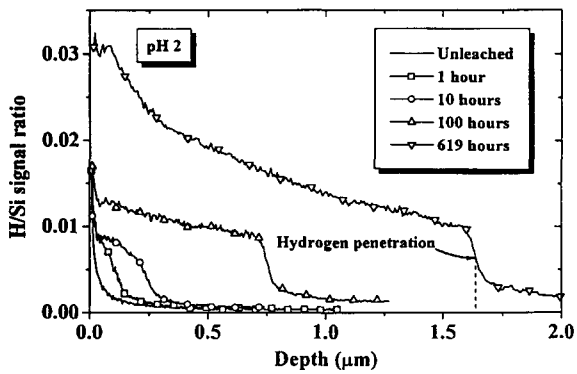


Fig. 5. SIMS hydrogen depth profiles of $Na_2O$–$0.2Al_2O_3$–$2.8SiO_2$ glasses leached in pH 2 solution at 25°C for up to 619 h.

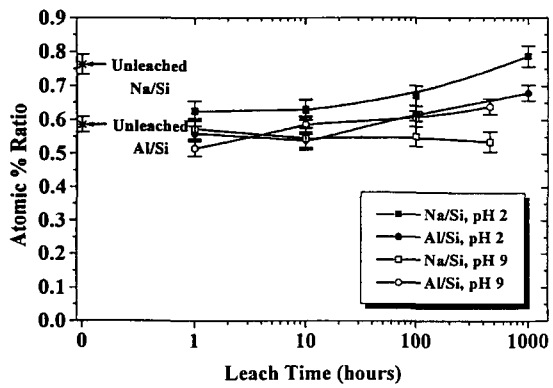


Fig. 7. XPS Na/Si and Al/Si atomic percent ratios as a function of leaching time for $Na_2O$–$0.8Al_2O_3$–$2.2SiO_2$ glasses leached in pH 2 and pH 9 solutions at 25°C. Lines are drawn as guides for the eye.

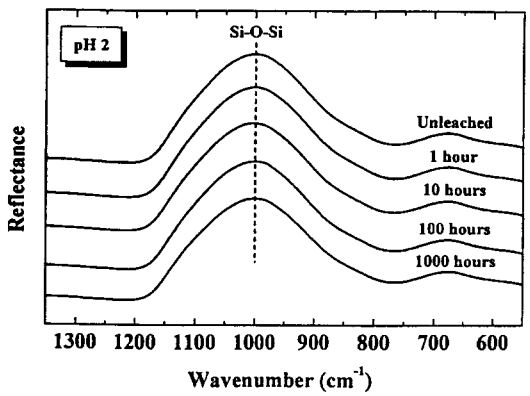


Fig. 8. FTIRR spectra of $Na_2O$–$0.8Al_2O_3$–$2.2SiO_2$ glasses leached in pH 2 solution at 25°C for up to 1000 h.

sodium, aluminum, or silicon.

### 3.2. $Na_2O$–$0.8Al_2O_3$–$2.2SiO_2$ glasses

The surface compositions of the 0.8 glasses, as measured with XPS, are illustrated in Fig. 7. These data indicate that there is little sodium and aluminum depletion in the glass surface in either acid or base at all leaching times. However, sodium depletion is slightly higher in base than in acid after long periods of time.

Fig. 8 shows the FTIRR spectra for the 0.8 glasses leached in acid. The peak associated with Si–O–Si bonds is located at $\approx 1000\ cm^{-1}$. There is no distinct peak associated with Si–O-modifier bonds in the 0.8 glasses (as observed in the 0.2 glasses) due to the lowered NBO concentration. Fig. 8 indicates no significant change in peak shape or position after 1000 h in acid indicating the absence of any surface layer formation. The FTIRR spectra for the glass in base (not shown here) indicate similar effects.

Table 2
ICP solution analysis of the 0.8 glasses leached in pH 2 solution

| Time | pH start | pH finish | Na (ppm) | Al (ppm) | Si (ppm) |
|---|---|---|---|---|---|
| 1 h | 1.98 | 1.99 | 0.20 | 0.10 | 0.13 |
| 10 h | 1.98 | 1.97 | 1.80 | 1.20 | 1.74 |
| 100 h | 1.98 | 2.02 | 8.50 | 7.80 | 10.94 |
| 1000 h | 1.88 | 2.41 | 64.00 | 58.00 | 80.90 |

SIMS depth profiles (not shown here) of the glasses leached in acid and base are identical to the unleached glass depth profiles, indicating no significant penetration of hydrogen or depletion or enrichment of sodium and aluminum. However, the depth sensitivity of SIMS depth profiling (with an $^{18}O^-$ primary beam) is limited to $\approx$ 200–500 Å; therefore, changes in the outermost 200–500 Å may not be apparent in the SIMS profiles.

Table 2 presents ICP spectrochemical analyses of the acid solutions. This data reveals significant dissolution of the glass network structure in acid. The Na/Si and Al/Si weight ratios in the solution were similar to those in the bulk glass at each time interval, indicating total dissolution of the glass network. Solution analyses of the base solutions did not detect the presence of sodium, aluminum, or silicon.

## 4. Discussion

The leaching and dissolution behavior of sodium-aluminosilicate glasses is strongly influenced by the NBO concentration. The bulk glass structures of the 0.2 and 0.8 glasses are quite different. The non-bridging oxygen concentration was not experimentally measured in this study. However, the NBO concentration was calculated based on the conventional model [7–11] that every Al ion (up to the ratio Na/Al = 1) enters the network and eliminates a non-bridging oxygen. Based on this calculation, the 0.2 and 0.8 glasses contain five and one non-bridging oxygen ions per 10 tetrahedra, respectively.

Smets and Lommen [12,13] suggested that Al ions begin to enter modifier sites at Na/Al ratios less than 1.0. Their model would suggest that the 0.8 glass has no non-bridging oxygens. They further claimed that Na ions bonded to non-bridging oxygens are more easily leached than Na ions bonded to the aluminum part of the network [13]. However, it also should be pointed out that the mobility of Na ions is increased by the addition of alumina [15].

XPS, SIMS and FTIRRS reveal that the 0.2 glass forms an extensive silica-rich, sodium de-

pleted layer in acid; the Al/Si ratio in the layer is less than the bulk value, suggesting some leaching of Al and/or structural transformation of the layer. In base, the sodium-depleted layer forms without a change in the Al/Si ratio. FTIRRS indicates that the structures of these layers contain fewer Si–O-modifier sites than the bulk glass due to the selective leaching of sodium ions from the surface, and/or due to transformation of the layer to a more condensed state.

FTIRRS and SIMS also indicate that the formation of a surface layer at pH 9 occurs at a rate that is one order of magnitude slower than at pH 2. From the hydrogen depth profiles, the 'effective' hydrogen diffusion coefficients in acid and base may be estimated through the relation

$$x = (Dt)^{1/2}, \tag{1}$$

where $x$ is the penetration depth in cm of hydrogen into the glass surface, $D$ is the effective diffusion coefficient in $cm^2/s$, and $t$ is time in s. The slope of a plot of $x^2$ vs. $t$ yields $1.17 \pm 0.20 \times 10^{-14}$ $cm^2/s$ and $1.62 \pm 0.20 \times 10^{-15}$ $cm^2/s$ as the effective hydrogen diffusion coefficients at pH 2 and pH 9, respectively.

The higher sodium leaching rate at pH 2 vs. pH 9 is most certainly due to a higher proton activity at pH 2, which supports Doremus' ion exchange model for the 0.2 glass. ICP solution analysis indicates that surface layer formation occurs without any detectable dissolution of the glass network structure in both acid and base.

XPS, FTIRRS and SIMS data show that no surface layer forms on the 0.8 glasses in acid. ICP solution analysis confirms that the glass network structure is dissolving, and since the relative amounts of Na, Al and Si in solution are stoichiometric with the glass composition, it can be concluded that the glass is dissolving congruently. The solution concentration of silicon (or other) glass species as a function of time at constant temperature can be expressed by the following equation as suggested by Lyle [16]:

$$Q = Kt^n, \tag{2}$$

where $Q$ is the quantity of silica released per unit surface area in $mol/cm^2$, $K$ is the extraction (or dissolution) rate constant in $mol/cm^2/s$, $t$ is time in s, and $n$ is a constant. A plot of log $Q$ as a function of log time indicated linear dissolution kinetics and the linear dissolution rate constant at pH 2 was calculated from the $y$-intercept as $K = 1.06 \pm 0.11 \times 10^{-10}$ moles $SiO_2/cm^2/s$.

The 0.8 glasses are resistant to the leaching of sodium ions from the network because most or all of these ions may be bonded to the aluminate species in the network. These sites presumably limit the release of sodium ions (even though their ionic mobility is high in the presence of alumina [15]). In acid, though, the aluminosilicate network dissolves (due to the acid solubility of $Al^{3+}$), and consequently, total dissolution is observed. In base, the aluminosilicate network seems to be much more stable, perhaps due to the limited solubility of $Al(OH)_3$. In contrast, the 0.2 glass exhibits extensive leaching of sodium ions in both acid and base. This supports the role of molecular water reactions in glasses with significant NBO concentration. The resulting surface layer, with a higher silica and lower alumina content, is stable in both pH 2 and pH 9 solutions.

This study shows that sodium concentration, alone, is not the determining factor in the glass corrosion behavior. Here, the $Na_2O$ concentration was held constant in two different aluminosilicate glasses to reveal the effects of glass structure. The effect of reducing the number of NBO sites in sodium-aluminosilicate glass networks is not only to increase the leaching resistance of sodium ions in both pH 2 and pH 9 solutions, but also to decrease the network dissolution resistance in pH 2 solutions. Clearly, the structural association of $Na^+$ with aluminate species in the glass lowers their effective activity to water reaction.

## 5. Conclusions

It has been shown that the leaching and dissolution behavior of sodium-aluminosilicate glasses is strongly influenced by the NBO concentration. The leaching and dissolution behavior of

$Na_2O$–$0.8Al_2O_3$–$2.2SiO_2$ and $Na_2O$–$0.2Al_2O_3$–$2.8SiO_2$ glass compositions, with structures containing one and five NBO sites per 10 tetrahedra, were investigated in pH 2 and pH 9 solutions at 25°C for up to 1000 h. The glass with five NBO sites per 10 tetrahedra exhibits extensive surface layer formation in both acid and base, which accounts for its resistance to network dissolution. The glass with one NBO site per 10 tetrahedra dissolves faster in acid than a distinct layer can form. In base, this glass is essentially unreactive as exhibited by very little sodium and no aluminum depletion as well as no network dissolution.

## Acknowledgements

The authors gratefully acknowledge the Department of Energy (DE-FG02-95ER14547.A000) for their financial support. We also thank Susan Brantley and Vince Bojan for stimulating discussion.

## References

[1] T.A. Wassick, R.H. Doremus, W.A. Lanford, C. Burman, J. Non-Cryst. Solids 54 (1983) 139.
[2] K.B. Harvey, C.D. Litke, J. Am. Ceram. Soc. 67 (1984) 553.
[3] R.H. Doremus, J. Non-Cryst. Solids 19 (1975) 137.
[4] B.M.J. Smets, T.P.A. Lommen, Phys. Chem. Glasses 24 (1983) 35.
[5] F.M. Ernsberger, Proc. XIV Int. Congr. on Glass, 1986, p. 319.
[6] I.S.T. Tsong, C.A. Houser, W.B. White, G.L. Power, J. Non-Cryst. Solids 38&39 (1980) 649.
[7] J.E. Shelby, J. Appl. Phys. 49 (1978) 5885.
[8] R. Brückner, H.-U. Chun, H. Goretzki, Glastech. Ber. 51 (1978) 1.
[9] G.W. Tasker, D.R. Uhlmann, P.I.K. Onorato, M.N. Alexander, C.W. Struck, J. Phys. (Paris) C8 (1985) 273.
[10] D.S. Goldman, Phys. Chem. Glasses 27 (1986) 128.
[11] C.H. Hsieh, H. Jain, A.C. Miller, E.I. Kamitsos, J. Non-Cryst. Solids 168 (1994) 247.
[12] B.M.J. Smets, T.P.A. Lommen, Phys. Chem. Glasses 22 (1981) 158.
[13] B.M.J. Smets, T.P.A. Lommen, Phys. Chem. Glasses 23 (1982) 83.
[14] F. Geotti-Bianchini, L.D. Riu, G. Gagliardi, M. Guglielmi, C.G. Pantano, Glastech. Ber. 64 (1991) 205.
[15] C.H. Hsieh, H. Jain, J. Non-Cryst. Solids 183 (1995) 1.
[16] A.K. Lyle, J. Am. Ceram. Soc. 26 (1943) 201.